PROGRESS WITH THE BOOSTER DESIGN FOR THE DIAMOND-II UPGRADE

I. P. S. Martin, C. Christou, M. Cox, R. T. Fielder, J. Kallestrup, A. Shahveh, W. Tizzano
Diamond Light Source, Oxfordshire, U.K
A. Brynes, J. K. Jones, B. Muratori, H. L. Owen, ASTeC, STFC Daresbury Laboratory, U.K

Abstract

Efficient injection into the Diamond-II storage ring [1, 2] will require an emittance and bunch length substantially below the values produced from the existing booster. Whilst an earlier design for a replacement based on TME cells was able to meet the target values of <30 nm.rad and <40 ps respectively [3, 4], several technical constraints have led to a rethink of this solution. The revised booster lattice utilises a larger number of cells based on combined-function magnets with lower peak fields that still meets the emittance and bunch length goals. In addition, the new ring has been designed to have low impedance to maximise the extracted charge per shot. In this paper we describe the main features of the lattice, present the status of the engineering design and quantify the expected performance.

INTRODUCTION

Diamond Light Source is developing the Technical Design Report for a major facility upgrade, at the heart of which is a replacement of the storage ring with a multi-bend achromat lattice [1, 2]. Efficient injection into the new storage ring will require upgrades to the injector complex, including a new 3.5 GeV low-emittance booster synchrotron with bunch length <40 ps at extraction. Maximising the charge per shot in both single and multi-bunch operation is also desirable to minimise the number of shots fired during top-up cycles, as well as to leave open the possibility of future single bunch swap-out operation in the storage ring. As such, a low-impedance vacuum chamber and raising the injection energy from 100 to 150 MeV both remain under consideration.

An early design for the replacement booster was able to deliver the required bunch parameters, albeit with a large number of magnets and demanding field parameters [3, 4]. A revised installation strategy also now envisages removal of the existing booster before installation of the new one inside the same tunnel, keeping the location of the main straight sections fixed. These two aspects have prompted a re-design of the lattice.

BOOSTER-II LATTICE

Lattice Design

The existing tunnel has a racetrack structure, leading to a new lattice with two arcs and two main straight sections. The original TME-style unit cells have been replaced with alternating focussing-defocussing combined function dipoles with integrated sextupole component for chromaticity correction. This results in a more efficient use of space, reducing
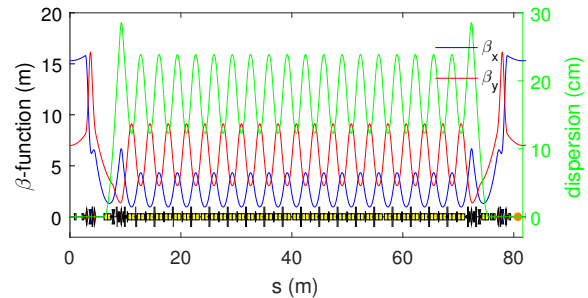
Figure 1: Twiss parameters for one super-period.

Table 1: Booster Parameters at Extraction

Parameter	Existing Booster	New Booster
Energy Range	0.1-3.0 GeV	0.1-3.5 GeV
Ramping frequency	5 Hz	5 Hz
# Cells	22	36
Circumference	158.4 m	163.846955 m
Betatron Tunes	[7.18, 4.27]	[12.20, 5.36]
Nat. Chromaticity	[-9.7, -6.3]	[-13.5, -12.0]
Emittance	134.4 nm.rad	17.7 nm.rad
Energy spread	0.073 %	0.086 %
Loss Per Turn	0.58 MeV	0.95 MeV
Nat. Bunch Length	99.3 ps	38.7 ps

the number of magnets and relaxing the field strengths. In addition, combined-function dipoles provide more control of the damping partition numbers, and the more compact lattice enables a further reduction in the emittance by increasing the number of cells from 28 to 36. Based on the results of a systematic scan, the cell tune was set to [0.280,0.104], as this was found to provide a good compromise between low emittance, low energy spread, low chromaticity and large horizontal and vertical dynamic aperture. The sextupole component in the combined-function dipoles is set to correct the operating chromaticity to [+2,+2], and trim sextupoles are distributed throughout the arcs to enable additional fine tuning and to counter the effects of eddy currents in the vacuum chamber walls.

At the ends of the arcs are two matching sections, each consisting of a normal dipole and a quadrupole doublet for dispersion suppression, along with quadrupole triplets for matching across the straights and for tune control. The optics for one super-period are shown in Fig. 1 and a summary of the ring and electron beam parameters at 3.5 GeV are given

in Table 1. The operating tune point remains under review depending on the results of emittance exchange studies [5,6].

Injection into the booster is to be single-turn and on-axis using one septum magnet and one injection kicker. Single-turn extraction is also assumed. In order to keep the kicker field below 0.1 T, three kickers are placed at the upstream end of the extraction straight and the septum positioned at the downstream end to maximise the separation. Due to space constraints, one of the five-cell RF cavities is placed between the final kicker and the extraction septum. Particle tracking studies confirm this arrangement has negligible impact on the extracted electron beam parameters. The injection and extraction kickers are assumed to be flat-top with fall/rise times of <0.2 μs respectively to allow multi-bunch trains of up to 180 bunches for 2 ns bunch separation.

Impact of Errors

Orbit correction in the booster assumes 48 BPMs, 48 horizontal correctors and 48 vertical correctors. Tune control is to be carried out by modifying the ramp profiles of the matching cell quadrupoles, and final chromaticity correction is to be achieved using the trim sextupoles. No other form of optics control is foreseen. The robustness of this strategy has been confirmed through particle tracking with AT2.0 [7] using the field and alignment errors given in Table 2. Errors were applied in a Gaussian distribution truncated to 2σ, the results of which are shown in Fig. 2. In addition to the magnetic errors, the impact of eddy currents [8] and varying the operating chromaticity in the range [+1,+1] to [+3,+4] was studied and confirmed as acceptable.

Table 2: Magnet Field and Alignment Errors (1σ)

Element	x/y (μm)	roll (μrad)	strength error
Dipole	100	200	2×10^{-3}
Quadrupole	50	200	5×10^{-3}
Sextupole	50	200	10×10^{-3}
Girder	150	150	-
BPM	500	-	-
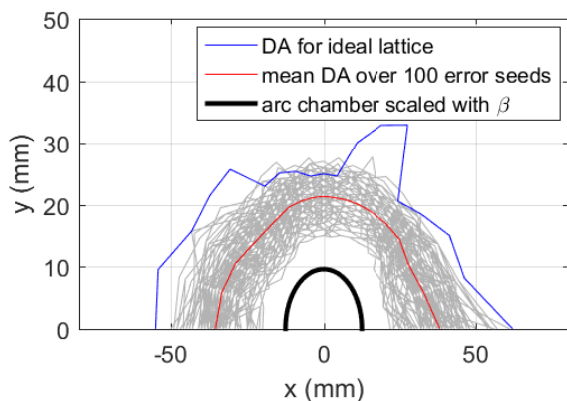
Figure 2: Dynamic aperture over 100 error seeds.

Collective Effects

Given the need to produce short, low-emittance electron bunches, possibly of up to 5 nC for a future single bunch swap-out operating mode, the impact of collective effects is a significant concern for Booster-II. This topic is currently under study using the ELEGANT tracking code [9], in which the effects of resistive wall and geometric impedances during the ramp can be studied alongside the impact of synchrotron radiation emission and intra-beam scattering. For these studies, the required geometric impedances have been calculated from the engineering models using CST Studio [10], and resistive wall effects have been included using analytic formulae for a circular pipe [11]. A summary of the main components and the resulting loss and kick factors for a 3 mm bunch are given in Table 3.

Alongside the development of a low-impedance vacuum chamber, raising of the injection energy from 100 MeV to 150 MeV by installing a third linac structure is also being considered. This is expected to benefit the operation in a number of ways, including:

- raising instability thresholds;
- reducing the dynamic range of the RF cavities and magnet power supplies;
- reducing eddy currents in the vacuum chamber;
- avoiding remanent fields at injection;
- minimising intra-beam scattering;
- lowering the geometric emittance and relative energy spread of the electron beam from the linac;
- increasing the gas lifetime

Experiments conducted into varying the injection energy into the existing booster support this expectation [12].

Table 3: Impedance Database

Component	No.	Total Loss Factor (V/pC)	Total Kick Factor (V/pC/mm)
BPM block	44	0.07	0.04
Pumping Cross	38	0.7	0.15
Ceramic Break	2	0.4	0.03
5-cell RF Cav.	2	5.2	0.003
HOM-damp Cav.	2	2.4	0.002
Screens	2	0.3	0.01
Striplines	2	0.16	0.02
Resistive Wall	140 m	7.4	1.8

ENGINEERING DESIGN

Vacuum Chamber

The vacuum chamber has been designed with a constant circular cross section of internal radius 11.9 mm through the arcs and 18.3 mm in the straight sections, thereby minimising the need for transitions and tapered sections. The chamber material will be stainless steel, with thicknesses of 0.5 mm, 0.7 mm or 1 mm under consideration. To maintain

RF continuity, a design for a combined pumping cross / bellows section with internal RF fingers and venting slots has been designed and prototyped (see Fig. 3). The magnets are to be supported on girders, with each girder supporting one focussing / defocussing dipole pair and connected to the next by the pumping cross.
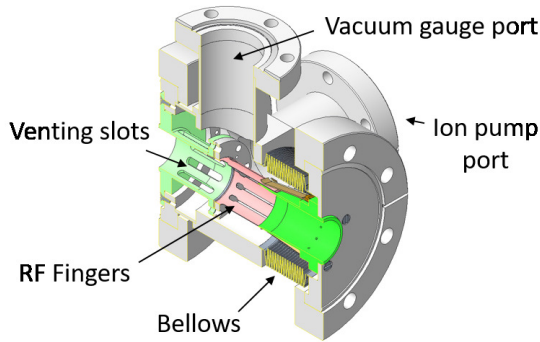
Figure 3: Pumping cross with integrated bellows.

One ceramic break 5 mm long is included in each arc to counter the transformer effect. The booster striplines have been designed to reduce the impedance and are identical to those planned for the storage ring [13, 14]. Diagnostic screen assemblies in the injection and extraction straights include a vacuum chamber insert to provide continuity when the screens are retracted, as shown in Fig. 4.
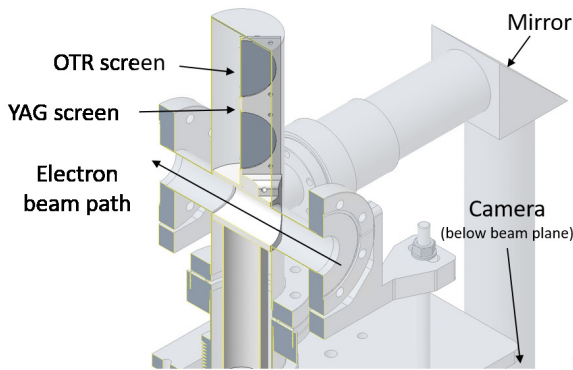
Figure 4: Diagnostic screen assembly (injection).

Magnets

A summary of the booster magnet parameters is given in Table 4. The design of these magnets is still in progress, however, two significant effects have been taken into account. The first relates to the different magnet lengths for each multipole component in the combined-function magnets, as shown in Fig. 5 for the focussing dipoles. This needs to be compensated for by adjusting the target quadrupole and sextupole components to recover the correct integrated strengths. In addition, an effective hard-edge model of the magnet needs to be constructed from the 3D model for inclusion in tracking codes. This can be achieved in several ways, for example using the procedure outlined in [15].

Table 4: Booster Magnet Parameters at 3.5 GeV

	BB	BD	BF	Quad	Sext
Length (m)	1.25	1.3	1.3	0.45	0.05
B-field (T)	0.95	0.99	0.42	-	-
Gradient (T/m)	-	-8.1	11.1	30	-
Sextupole (T/m^2)	-	-43.8	36.9	-	300
Radius (mm)	13.6	13.6	13.6	20.4	13.6
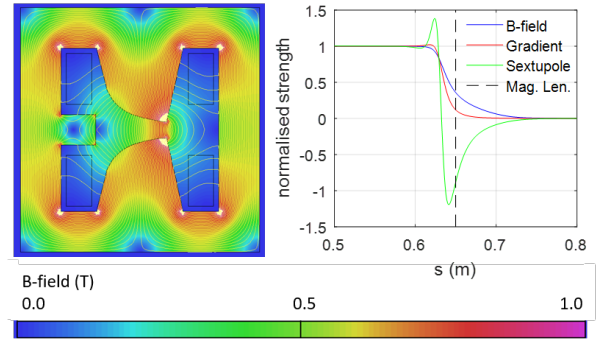
Figure 5: OPERA magnet model for the BF dipoles (left) and multipole components along the beam path (right).

The second effect is that of saturation and remanent fields in the magnets. For the single-function magnets these effects can be compensated by simply adjusting the driving power supply waveforms. For the combined-function magnets however, the three multipole components diverge and only the dipole term can be corrected using the magnet power supply. A strategy to stabilise the resulting tunes and chromaticity shifts during the ramp by using the single-function magnets remains to be developed.

RF

To replace the losses from synchrotron radiation and achieve the required bunch length at extraction, a peak RF voltage of 2.0 MV needs to be provided. This is to be achieved by reusing the two five-cell normal conducting cavities from the existing booster [16]. For contingency, two of the same single-cell HOM-damped cavities as currently installed in the storage ring [17] will also be installed. In all cases, the cavities will be powered using solid-state amplifiers and regulated by a digital low-level RF system [18].

CONCLUSIONS

The design of the replacement booster for the Diamond-II project is well advanced. The proposed solution meets the top-level design goals needed to ensure efficient injection into the new storage ring, and the maximum single and multi-bunch charge per shot is under study.

In addition to the changes outlined here, modifications to both the linac-to-booster (LTB) and booster-to-storage ring (BTS) transfer lines will be required. These include additional magnets for matching purposes and a revised layout to match to the new injection and extraction points.

REFERENCES

[1] "Diamond-II Conceptual Design Report", Diamond Light Source, 2019, `https://www.diamond.ac.uk/Home/About/Vision/Diamond-II.html`

[2] H. Ghasem, I. P. S. Martin, B. Singh, and R. P. Walker, "Progress with the Diamond-II Storage Ring Lattice", in *Proc. IPAC'21*, Campinas, Brazil, May 2021, paper THPAB090, this conference.

[3] I. P. S. Martin and R. Bartolini, "Conceptual Design of an Accumulator Ring for the Diamond II Upgrade", *J. Phys.: Conf. Ser.*, vol. 1067, p. 032005, 2018. `doi:10.1088/1742-6596/1067/3/032005`

[4] I. P. S. Martin *et al.*, "Injection Studies for the Proposed Diamond-II Storage Ring", in *Proc. IPAC'19*, Melbourne, Australia, May 2019, paper WEPMP043, pp. 2430–2433.

[5] P. Kuske and F. Kramer, "Transverse Emittance Exchange for Improved Injection Efficiency", in *Proc. IPAC'16*, Busan, Korea, May 2016, paper WEOAA01, pp. 2028–2031.

[6] J. Kallestrup and M. Aiba, "Emittance Exchange in Electron Booster Synchrotron by Coupling Resonance Crossing", *Phys. Rev. Accel. Beams*, vol. 23, p. 020701, Feb. 2020. `doi:10.1103/PhysRevAccelBeams.23.020701`

[7] Accelerator Toolbox, ATCOLLAB, version 2.0, `https://atcollab.github.io/at/`.

[8] M. Munoz and W. Joho, "Eddy Current Effects in the SLS Booster", Paul Scherrer Institute, SLS-TME-TA-1998-0010, Oct. 1998.

[9] M. Borland, "elegant: A Flexible SDDS-Compliant Code for Accelerator Simulation", Advanced Photon Source, LS-287, Sept. 2000.

[10] CST Studio Suite, Dassault Systemes, `https://www.3ds.com/products-services/simulia/products/cst-studio-suite/`.

[11] T. Olsson and R. T. Fielder, "Single-Bunch Thresholds for the Diamond-II Storage Ring", in *Proc. IPAC'21*, Campinas, Brazil, May 2021, paper MOPAB072, this conference.

[12] I. P. S. Martin *et al.*, "Open Questions for the Diamond-II Booster", in *28th European Synchrotron Light Source Workshop*, ESRF, Grenoble, France, Dec. 2020.

[13] A. Morgan, "Multi-Bunch Feedback Kickers for Diamond-II", in *DLS-2 / SLS 2.0 Information Exchange*, Nov. 2020, `https://indico.psi.ch/event/10519/`.

[14] R. T. Fielder and T. Olsson, "Construction of an Impedance Model for Diamond-II", in *Proc. IPAC'21*, Campinas, Brazil, May 2021, paper MOPAB127, this conference.

[15] D. Einfeld *et al.*, "Modelling of Gradient Bending Magnets for the Beam Dynamics Studies at ALBA", in *Proc. PAC'07*, Albuquerque, New Mexico, Jun. 2007, paper TUPMN068, pp. 1076-1078.

[16] "Data Sheet: 500 MHz, 5-Cell Cavity", DESY-MHFe v. 2.1, Oct. 2007.

[17] E. Weihreter, "Status of the European HOM-Damped Normal Conducting Cavity", in *Proc. EPAC'08*, Genoa, Italy, June 2008, paper THXM03, pp. 2932-2936.

[18] C. Christou *et al.*, "RF Plans for the Diamond-II Upgrade", in *Proc. IPAC'21*, Campinas, Brazil, May 2021, paper MOPAB107, this conference.